P3.5 Changes in the Intraseasonal Variability of Precipitation over the United States Associated With ENSO

David Small and Shafiqul Islam*
University of Cincinnati

1. Introduction

In order to accurately assess the potential impact of a possible climate change on patterns of precipitation variability, it is important to first understand and quantify the characteristics of natural fluctuations in precipitation. Land-atmosphere-ocean interactions include a variety of feedbacks that have time scales of years or longer, producing a range of low frequency variations in atmospheric variables. One well-known mode of natural variability is associated with El-Nino/Southern Oscillation (ENSO), a coupled mode to the ocean and atmosphere that is known to influence the space-time variability of precipitation and temperature in different regions of the globe.

The relationship between sea surface temperature anomalies associated with ENSO and changes in seasonal or annual precipitation is well documented in the scientific literature. Relatively few studies have considered changes in the intraseasonal characteristics of precipitation variability between El Nino (La Nina) events and neutral winters. In this paper, changes in the intraseasonal characteristics of precipitation associated with ENSO are investigated and their significance estimated.

Most studies have identified changes in the intraseasonal variance of precipitation or temperature after pooling temperature or precipitation data to form a composite of El Nino, La Nina or neutral years. Pooling the data in this fashion ignores the possibility of shifts in the mean between individual El Nino or La Nina years that may or may not be related to SST anomalies. The significant event-to-event differences in the magnitude and location of SST anomalies and large year-to-year variability of precipitation must also be considered when assessing the significance of changes in the variance. To avoid overestimating the impact of ENSO on intraseasonal variability, the significance of changes in the variance must be estimated by considering precipitation anomalies from each event separately.

Precipitation possesses significant variability on daily, synoptic, monthly and subseasonal time scales, each of which may be dominated by a different dynamical mechanism. If the changes in precipitation during ENSO events are scale-dependent, it is important to identify the dominant timescale so that a physical mechanism can be assigned to the observed changes.

In this paper, Granger causality analysis is used to identify regions in the United States where there exists a statistically significant causal relationship between SST anomalies, as captured by the Nino-3.4 index, and changes in the seasonal precipitation totals. After determining that lagged values of the SST anomalies contain significant information about the current state of precipitation anomalies, the precipitation timeseries from each gridpoint in the daily precipitation dataset are separated into the 9 strongest El Nino, La Nina and 9 most neutral winters based on the sign and magnitude of the Nino-3.4 index.

If there exists a significant relationship between seasonal precipitation anomalies and SST anomalies in a region of the United States, is the probability of observing an increase or decrease in the seasonal mean or intraseasonal variance is greater during a warm (El Nino) or cold (La Nina) event than in any of the other winters in the dataset? To explore this question, anomalies in the mean or variance are calculated for each of the winters in the dataset by subtracting the neutral winter average estimated by pooling all of the neutral winters together. The number of winters for which the mean or variance is larger or smaller than the neutral winter average is tabulated and the significance of the probabilities of observing an increase or decrease is estimated by the Fisher exact test using the hypergeometric distribution.

Given a significant probability of observing an increase or decrease in the variance during ENSO events, do increases or decreases in the variance exhibit a characteristic timescale or does the variability change across scales? To explore this possibility, the timeseries are decomposed with the maximal overlap discrete wavelet transform (MODWT) and the variance estimated at intraseasonal timescales ranging from 2 days to 64 days. This provides an estimate of changes in the variance on synoptic (4 to 16 days), monthly (16 to 32 days) and subseasonal (32 to 64 days) timescales, all of which can be associated with known physical processes in the climate system.

2. Previous Studies of ENSO-Related Variability

When considering the variability of precipitation, many different estimates of the dominant timescale of intraseasonal variability have been offered

Using a gridded dataset of daily precipitation, Ye and Cho (2001) found two distinct scales of intraseasonal oscillations in precipitation, one around 37 days and the other around 24 days, that each explained 11% of the variance. Analyzing the same gridded dataset with a combination of the discrete wavelet transform and principal component analysis, Joseph et al. (2000) found that four different timescales of variability explain

* Corresponding author address: Dr Shafiqul Islam, University of Cincinnati, Cincinnati Earth Systems Science Program, Dept. of Civil and Environmental Engineering, Cincinnati, OH, 45221; e-mail: islams@email.uc.edu.

most of the spatial fluctuations in precipitation. They found that the dominant scales of variability were the synoptic (16 hours to 22 days) explaining 40.13% of the spatial variance, seasonal (43 to 341 days) explaining 30.5% of the variance, subdiurnal (2 to 16 hours) explaining 20.72% of the variance and climatic scales (longer than 2 years) explaining 5.33% of the variance. They also report strong seasonal variations in these patterns, with the fluctuations in winter being dominated by synoptic scale variability and those in summer by subdiurnal scale variability.

The physical mechanisms behind anomalous precipitation act on many different time and space scales. Low frequency variability in the atmosphere, either that associated with known climate oscillatory processes or decadal variability, is known to influence the patterns of precipitation in space and time.

Though most of the variance in precipitation is on timescales much shorter than a month, the majority of studies focusing on the variability of precipitation have used monthly, seasonal or yearly data. Del Sole (2001) suggests that anomalies in monthly averages of geopotential height may arise from a few episodes lasting less than a few weeks that dominate the variance by means of their large amplitudes rather than their persistence. Several recent studies suggest that the characteristic timescales for a number of low frequency oscillations in the atmosphere, as measured by their e-folding time, may be on the order of several days.

Compo et al. (2001) find that the effect of ENSO on 500-mb geopotential height variability depends strongly on the time scale used for the analysis. In particular, the spatiotemporal patterns of variability on the synoptic (2 to 7 days), intra-seasonal (8 to 45 days) and monthly timescales are all sharply different. In some regions, the variability of height anomalies on the synoptic scale differ in sign with those on intra-seasonal scales canceling out in large area averages and leading to insignificant sub-seasonal variability. Anomalies in the daily NCEP reanalysis product precipitation data were found to be scale independent. (Compo et al., 2001)

DelSole (2001), using a measure of the decorrelation time to find patterns in space that maximize the e-folding time of the correlation function of daily anomaly fields of the 500 hPa geopotential height, found that the maximum decorrelation time associated with the Arctic Oscillation is on the order of 12 to 15 days.

Feldstein (2000), analyzing daily 300-mb geopotential height data from the NCAR-NCEP reanalysis data product between 1958 and 1997, suggests that the temporal evolution of the North Atlantic Oscillation, Pacific North America and West Pacific teleconnection patterns, but not ENSO, can be interpreted as Markov Processes with characteristic time scales between 7.4 and 9.5 days. Using spectral analysis, Feldstein found evidence of an oscillation with a period of about 20 days in the daily ENSO teleconnection pattern.

These findings suggest that anomalies in monthly or seasonal averages associated with global teleconnections may arise from a few episodes lasting less than a couple of weeks that dominate the variance by means of their large amplitudes rather than their persistence. To explain a majority of the variance associated with such globally active teleconnections, daily or finer data should be used.

Kumar and Hoerling (1997) suggested that the observed spatial patterns of the extratropical circulation anomalies normally associated with ENSO are not a deterministic function of SST anomalies. They investigated the observed event-to-event variability of ENSO by averaging the 500-mb geopotential height anomalies from the 7 strongest El Nino events during the period from 1950 to 1994 to form a composite response. Their results showed that the response of each individual event differed substantially from the composite, demonstrating the importance of examining precipitation anomalies observed during each event separately.

3. Data

For this study, daily precipitation timeseries from individual gages as well as data from a finely gridded dataset was analyzed. The gridded data, on a 0.25° longitude x.25° latitude grid, is part of the Daily US UNIFIED Precipitation dataset provided by the NOAA-CIRES Climate Diagnostics Center. The dataset covers the period January 1, 1948 to December 31, 1998 and includes 50 winters (DJF) with 9 each of El Nino and La Nina events. There are more than 13000 station reports each day for 1948-1991 and about 8000 from 1992 on. The dataset, complete for the 50 years, contains 13726 points on the land surface.

The data is divided into individual winter and then further subdivided into El Nino, La Nina and neutral seasons based on the average monthly Nino-3.4 index for each particular season and year. (Mason and Goddard, 2001). Those seasons with sea surface temperature anomalies greater than 0.5 °C are classified as El Nino while those with magnitudes less than -0.5 °C are classified as La Nina. All seasons with sea surface temperature anomalies between -0.5 °C and 0.5 °C are classified as neutral. To make comparisons between seasons and different phases of ENSO easier, only the 9strongest El Ninos and La Ninas and 9 most neutral events (smallest sea surface temperature anomalies) for each season were considered in the analyses.

4. Methods and Results

4.1 Granger Causality Analysis

The Granger causality between the Nino-3.4 SST and seasonal precipitation anomalies is estimated over the United States using the procedure described by Kaufmann and Stern (1997). Granger causality is an improvement over lagged correlation analysis, which suffers in the presence of autocorrelation between fields, though it is no more able to imply a physical reason for the statistical relationship.

The procedure consists of two steps. In the first, two-way interactions between the monthly SST anomaly and the monthly precipitation anomaly at each gridpoint are estimated using the following vector autoregression (VAR) model evaluated with s time lags

$$P_i = \alpha_{1i} + \sum_{i=1}^{s} \beta_{1i} P_{i-1} + \sum_{i=1}^{s} \gamma_i SST_{i-1} + e_{1i}$$

$$SST_i = \alpha_{2i} + \sum_{i=1}^{s} \beta_{2i} P_{i-1} + \sum_{i=1}^{s} \gamma_{2i} SST_{i-1} + e_{2i} \quad (1)$$

where the α's, β's and γs are regression coefficients and the e's are error terms.

To establish causality between the SST and precipitation anomalies, the VAR model is estimated again after removing the causal variable. To test whether the Nino-3.4 SST anomalies cause variability in precipitation totals, the model is estimated again removing the lagged SSTs from the precipitation equation as follows:

$$P_i = \alpha_{1i} + \sum_{i=1}^{s} \beta_{1i} P_{i-1} + e_{1i} \quad (2)$$

To estimate whether the restricted model is significantly different from the unrestricted estimate, we calculate a test statistic that can be evaluated with an F distribution,

$$\lambda = \frac{\left(RSS_r - RSS_u\right)/s}{RSS_u/\left(T - k\right)} \quad (3)$$

in which RSS is the squared sum of the residuals, T is the number of observations, k is the number of regressors in the unrestricted model and s is the number of time lags used. The subscripts r and u refer to the restricted and unrestricted models respectively. The null hypothesis that the eliminated variable does not cause variability in the dependent variable (seasonal total) can be estimated by comparing the test statistic with an F statistic with s and T-k degrees of freedom in the numerator and denominator respectively. We reject the null hypothesis of no causal order for values of λ with a probability greater than 0.05. If the null hypothesis can be rejected, it can be concluded that the lagged values of SST contain information about the current value of precipitation beyond that of the lagged precipitation alone.

To estimate the causal relationship between winter seasonal precipitation total and the average winter SST anomaly, Granger causality analysis was performed using seasonal totals and seasonal averages of the Nino-3.4 anomaly.

$$P_{W_i} = \alpha_{1i} + \sum_{i=1}^{s} \beta_{1i} P_{W_{i-1}} + \sum_{i=1}^{s} \gamma_i SST_{W_{i-1}} + e_{1i}$$

$$SST_{W_i} = \alpha_{2i} + \sum_{i=1}^{s} \beta_{2i} P_{W_{i-1}} + \sum_{i=1}^{s} \gamma_{2i} SST_{W_{i-1}} + e_{2i} \quad (4)$$

In this case, the variable under consideration is winter precipitation and the lagged values are fall (lag 1), summer (lag 2) and spring (lag 3).

The model was fit using seasonal totals, regressing winter precipitation anomalies first against fall and summer SST and precipitation anomalies and then against those from the previous fall, summer and spring (Figure 1.). When considering only the previous fall and summer, we find a significant causal relationship at 17.5% of the gridpoints, covering Florida and the southwest and an area along the southern edge of the country stretching from the southwest to the southeast. When considering spring as well, the same areas of the country demonstrate a significant relationship between SST and precipitation covering 15.8% of the gridpoints.

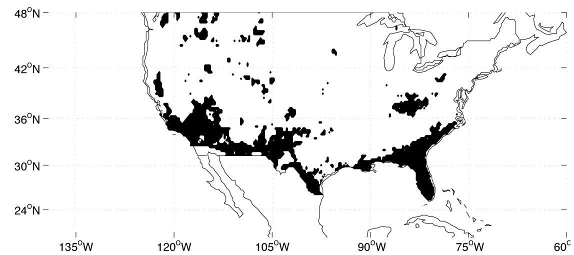

Figure 1. Areas with a statistically significant causal relationship between SST and winter precipitation.

Having identified a region that demonstrates a causal relationship between the SST temperature anomalies and seasonal precipitation totals, significance of changes in the mean and variance between El Nino, La Nina and neutral winters based on the magnitude of the SST anomalies is estimated.

4.2 Changes in the Mean and Variance

The daily values from all the El Nino, La Nina and neutral winters are pooled and a mean and process variance calculated for each type of event. Figure 2 shows the ratio of the El Nino to neutral and La Nina to neural mean and Figure 3 the same for the variance.

We find that at gridpoints where the mean increases (decreases) during El Nino winters, it decreases (increases) during La Nina winters, with increases in the southwest and southern Florida during El Nina winters and decreases along the northern half of the country and through the Ohio Valley. The opposite pattern is observed during La Nina winters with small increases along the northern part of the country and a large increase in the Ohio Valley. The changes in the variance are similar to the changes in the mean, with the largest changes occurring in the southwest and along the Gulf coast in El Nino winters and in the Ohio Valley region during La Nina winters.

To assess the statistical significance of the changes in the mean or variance between the ENSO winters and neutral winters, the Fisher exact test (Mason and Goddard (2001) is applied to estimate the probability of selecting 9 winters at random (the 9 strongest El Nino winters for example) out of the 50 in the dataset that have a positive anomaly in the mean or variance, where a seasonal anomaly is defined as the difference between the mean or variance in any individual winter and the neutral winter mean or process variance calculated by pooling all the events together. The test is used to estimate the significance of an increase or decrease in the mean or variance, not the magnitude of the change.

Figure 2 shows the results of the Fisher exact test for statistically significant increases in the mean and variance for El Nino winters ($p<0.05$). During El Nino winters, approximately 23.4 percent of the gridpoints experience a positive seasonal anomaly in the mean while the variance increases at 13.8 percent of the gridpoints. We find no large, spatially coherent regions with statistically significant changes in the mean or variance during La Nina winters or decreases during El Nino winters. We also find no statistically significant changes ($p<0.05$) between individual neutral winters and the neutral year average for either the mean or the variance, suggesting that the neutral winter average adequately captures the neutral winter characteristics.

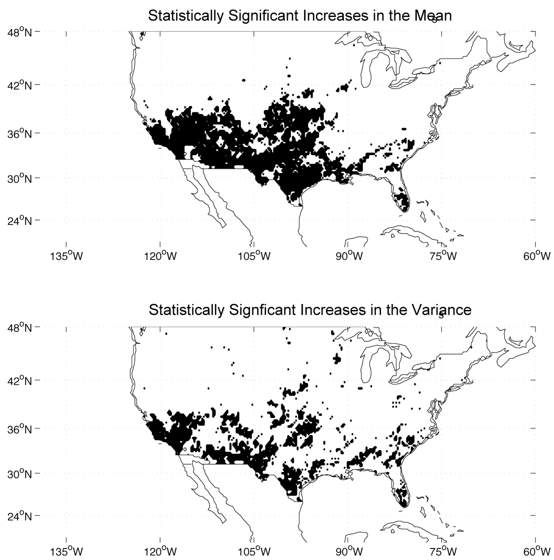

Figure 2. Statistically significant increases ($p<0.05$) in the mean and variance during El Nino winters evaluated with the Fisher exact test.

4.3 Wavelet Analysis of Variance

The discrete wavelet transform (DWT) is a signal processing technique that offers several advantages over traditional spectral analysis techniques. The DWT has the advantage of being scale adaptive, allowing the precipitation time series to be decomposed into a collection of new time series, each of which represents the variability in the signal over a characteristic band of scales (e.g., subdiurnal, synoptic, intra-seasonal, etc.)

The wavelets form an orthonormal basis and are obtained by the translation and dialation of a mother wavelet, $\psi(t)$, such that

$$\psi_{n,m}(t) = \frac{1}{\sqrt{2^n}}\,\psi\left(\frac{t - m2^n}{2^n}\right) \tag{5}$$

The series expansion of a function, f(t), is

$$f(t) = \sum_{n} \sum_{m} D_{n,m}\psi_{n,m}(t) \tag{6}$$

where the summation is taken over all scales, n, and all translations, m. The wavelet coefficients, $D_{n,m}$, capture the variability of the timeseries at time $t = m2^n$ and scale $\lambda = 2^n$. (Joseph et al. 2000) Because the wavelets form a linear basis, a wavelet spectrum can be defined that represents the total energy (variance) at each frequency λ,

$$E_n = \sum_{m} \left|D_{n,m}\right|^2 \tag{7}$$

Unlike Fourier coefficients, which capture variability over the entire timeseries, the DWT captures variability associated with local features in a timeseries, producing a better estimate of the variance attributable to local, intermittent variations in a timeseries. The DWT can also be used to analyze timeseries data that is not stationary, one of the primary limitations of Fourier analysis. Unfortunately, the length of a timeseries must be of length 2N where N can be any integer. In this application, the timeseries from each gridpoint are not of a dyadic length, with the 51 years of data containing 18627daily values.

Rather than zero padding or arbitrarily truncating the timeseries, which due to the episodic nature of precipitation may potentially exclude one or more periods of precipitation, we apply the maximum overlapping discrete wavelet transform (MODWT), sometimes called the stationary or shift invariant wavelet transform to analyze the variance.

The MODWT provides several advantages over the DWT. It is able to decompose timeseries of arbitrary length. It is shift invariant, a circular shift of the original timeseries results in a corresponding shift of the MODWT scaling and wavelet coefficients, so the choice of starting point in a timeseries doesn't affect the analysis. The detail and approximation coefficients from the MODWT analysis are associated with a zero-phase filter making it possible to line up features in the original timeseries with those at different scales. The MODWT can also be used to analyze the variance in a timeseries as a function of timescale, but has been shown to be a more efficient estimator than the DWT. (Percival and Mofjeld, 1997).

The la8 wavelet is used to decompose the 50 year timeseries into 6 intraseasonal timescales representing variability on scales of 2, 4, 8, 16, 32 and 64 days. The timeseries of wavelet coefficients for each scale is then circularly shifted by the proper number of days to line up features in the coefficients with the same features in the original timeseries. The advantage of using the la8 wavelet is that it is is designed to be an approximately zero phase filter and is a particularly efficient estimator of the variance. (Percival and Mofjeld, 1997) The variance is first calculated at each scale by pooling all of the wavelet coefficients for the El Nino, La Nina and neutral winters and then separately for each winter in the dataset.

The Fisher exact test is used to estimate the significance of the difference of the variance between the El Nino or La Nina winters and the neutral winter average (Figure 3).

Figure 3 shows regions with statistically significant increases in the variance for scales 3 (8 days) and 5 (32 days) representing synoptic and monthly scale variability. Statistically significant increases are found at 13.6, 13.2,10.8, 11.4, 11.7 and 6.7 percent of the gridpoints for scales of 2 days, 4 days, 8 days, 16 days, 32 days and 64 days respectively. The increases occur in the same regions previously identified as possessing a significant Granger causal relationship between the seasonal total and SST anomalies as well as an increase in the total variance.

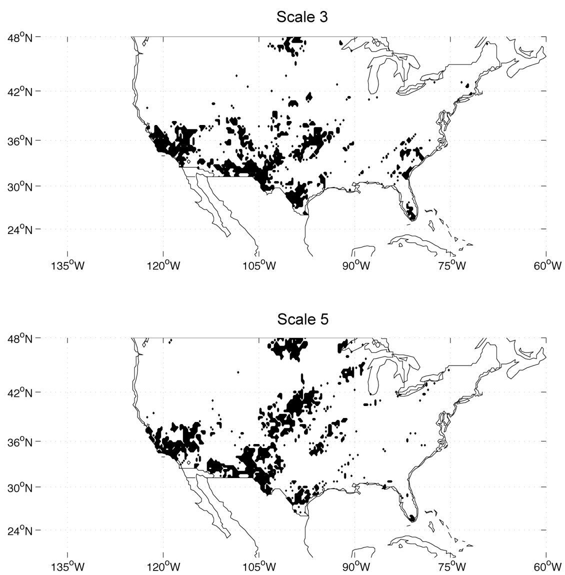

Figure 3. Statistically significant increases in the El Nino winter variance for MODWT scales 3 (8 days) and 5 (32 days).

5. Discussion

By applying Granger causality analysis to test for statistically significant causality between SST anomalies and seasonal precipitation total, we identified a region covering 17.5 percent of the land surface when we regressed winter precipitation and SST anomalies with a maximum lag of 2 seasons, fall and summer.

Having identified a region in the southwest, southern California, Florida and the Gulf Coast where the lagged SST anomalies contain significant information about the current state of the seasonal anomaly, we divided the daily precipitation timeseries into El Nino, La Nina and neutral winters based on the magnitude of the SST anomaly. We find that the mean and variance of precipitation increase during El Nino winters across the southern half of the country and decreases across the northern half of the country with an opposite pattern observed during La Nina winters. The changes are consistent with the results of previous studies that have found an increase in blocking over the North Pacific (Mullen 1989) decreasing the frequency of cyclones in the northwest during El Nino winters.

We applied the Fisher exact test to assess the significance of the sign of seasonal precipitation anomalies at each gridpoint in the gridded dataset. The exact test calculates the probability of drawing N winters with an anomaly of a given sign out of a sample of 9 winters given that M out of 50 winters also had a change of the same sign. Using this analysis, we find that 23.4 percent of the gridpoints experienced a statistically significant increase in the mean and 13.8 percent experienced an increase in the variance with a 95 percent level of confidence. We find no spatially coherent decreases in the mean or variance during La Nina winters and no large-scale pattern of significant changes of either sign during La Nina winters. No statistically significant changes in the mean or variance were found for the 9 individual neutral winters used in the analysis.

The results of this study suggest that precipitation characteristics over a small area of the United States are affected by Nino-3.4 SST anomalies. Hypothesis testing suggests that given a large amount of year-to-year variability, a large event-to-event variability in ENSO and the small number of events on the record, a small area, between 11 and 13 percent of the land surface of the United States, experiences a robust increase in the variance of daily precipitation during El Nino winters. A MODWT analysis of variance suggests that the changes occur across timescales, suggesting that ENSO increases the daily, synoptic, monthly and subseasonal variance of daily precipitation.

6. References

Compo, G. P., Sardeshmukh, P.D. and Penland, C., 2001: Changes of Subseasonal Variability Associated with El Nino, *J. Climate*, **14**, 3356-374.

Del Sole, T., 2001: Optimally Persistent Patterns in Time-Varying Fields, *J. Atmos. Sci.*, **58**,11, 1341-1356.

Feldstein, S., 2000: The Timescale, Power Spectra and Climate Noise Properties of Teleconnection Patterns, *J. Climate*, **11**, 4430-4340.

Joeseph, R., Ting, M. and Kumar, P., 2000: Multiple-Scale Spatio-Temporal Variability of Precipitation over the Coterminous United States, J. Hydrometeor, 1, 373-392.

Kaufmann, R.K. & Stern, 1997: Evidence For Human Influence On Climate From Hemispheric Temperature Relations, *Nature* **388**, 3, 1997, 39-46

Mason, S.J. and Goddard, L., 2001: Probabilistic Precipitation Anomalies Associated with ENSO, *Bull. Amer. Meteor. Soc.*, **82**, 4, 619-637.

Percival, D.B. and Mofjeld, H.O., 1997: Analysis of Subtidal Coastal Sea Level Fluctuations. *J. Am. Stat. Assn.*, **92**, 439, 868-80.

Ye, H. and Cho, H. R., 2001: Spatial and temporal characteristics of intraseasonal oscillations of precipitation over the United States, *Thoer. and Appl. Climatol.*, 68, 51-66.